Biomacromolecules

Article

Cite This: Biomacromolecules 2018, 19, 3936−3944

pubs.acs.org/Biomac

Complex Coacervates between a Lactose-Modified Chitosan and Hyaluronic Acid as Radical-Scavenging Drug Carriers

Federica Vecchies,[†] Pasquale Sacco,*[,†] Eva Decleva,[†] Renzo Menegazzi,[†] Davide Porrelli,[‡] Ivan Donati,[†] Gianluca Turco,[‡] Sergio Paoletti,[†] and Eleonora Marsich[‡]

[†]Department of Life Sciences, University of Trieste, Via L. Giorgieri 5, I-34127 Trieste, Italy

[‡]Department of Medicine, Surgery and Health Sciences, University of Trieste, Piazza dell'Ospitale 1, I-34125 Trieste, Italy

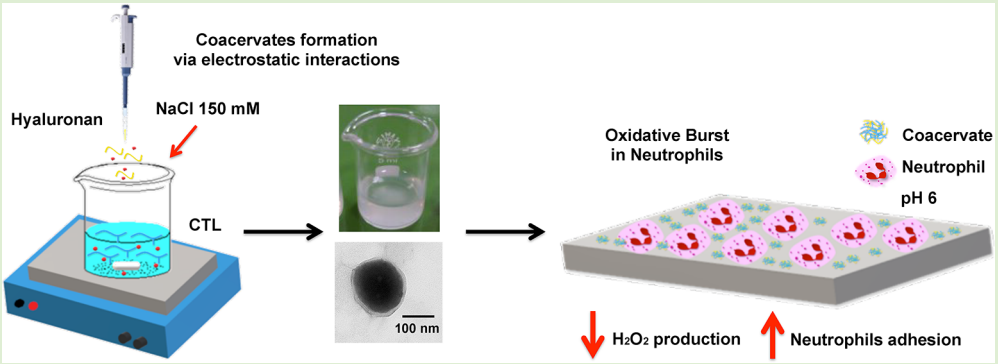

ABSTRACT: Complex coacervation of two oppositely charged polysaccharides, namely a lactose-modified chitosan (CTL) and hyaluronan (HA), was investigated in this study. Coacervates of the two polysaccharides were prepared by drop-by-drop injection of HA into CTL. Transmittance and dynamic light scattering (DLS) measurements in combination with TEM analyses demonstrated the formation of spheroidal colloids in the nano-/microsize range showing good homogeneity. Strikingly, the presence of 150 mM supporting NaCl did not hamper the colloid formation. Stability studies on selected formulations demonstrated that HA/CTL coacervates were stable up to 3 weeks at 37 °C and behaved as pH-responsive colloids since transition from entangled to disentangled chains was attained for a proper pH range. The possibility of freeze-drying the coacervates for storage purposes and the ability of encapsulating selected payloads were investigated as well, for two values of the fraction of the lactitol side-chain substitution (F_L). Finally, biological tests using human neutrophils were undertaken at acidic pH value (pH = 6.0): under such experimental conditions, akin to those frequently occurring in the inflammatory microenvironment, coacervates scavenged reactive oxygen species (ROS) generated by these cells in basal conditions. Given the well documented bioactivity of CTL with respect to chitosan toward cartilage regeneration, these findings point to a possible application of HA/CTL-based colloids as scavenging and bioactive carriers for the delivery of therapeutic molecules at confined inflamed sites such as knee joints.

1. INTRODUCTION

Ionically cross-linked colloidal polyelectrolyte (PE) complexes in the nano-/micro size range have been investigated in the last years as potential vehicles for the delivery of therapeutic molecules.[1] Specifically, the mixing of solutions containing oppositely charged PEs leads, under appropriate conditions, to a liquid−liquid phase separation; this process results in a biphasic system where the dense (PE-rich) liquid phase, the "coacervate", is in equilibrium with the PE-poor solution phase. This phenomenon is widely known as "complex coacervation"; it slightly differs from the simple "coacervation" process, in which a single PE is involved.[2,3] The attractive electrostatic forces, together with the entropy gain due to counterion and water release from PEs, play the key role for PEs association. The onset of complex coacervation can be then modulated by tuning physical−chemical parameters such as ionic strength, temperature, pH, charge density, molecular weight, and weight ratio of the two interacting PEs. The chemical mechanisms and conditions for PEs complex coacervation have been widely explored by different authors.[4−7]

Several examples of PEs coacervates—mostly conceived for biomedical applications—are reported in the literature. For instance, chitosan/nucleic acid polyplexes were designed for the *in vitro* delivery of RNA or DNA in mammalian cells.[8−10] Similarly, hybrid PEGylated nanoparticles formed via the complex coacervation mechanism have been shown to enhance the *in vivo* gene transfection efficiency compared with traditional carriers.[11] On the other hand, protein encapsulation via polypeptide complex coacervation has been recently reported with the aim of delivering protein therapeutics.[12]

Received: June 1, 2018
Revised: August 6, 2018
Published: September 11, 2018

DOI: 10.1021/acs.biomac.8b00863
Biomacromolecules 2018, 19, 3936−3944

In the context of drug delivery and tissue engineering, polycation/polyanion polysaccharide complex coacervation has been widely explored by several research groups.[13−17] Although various anionic biopolymers (e.g., alginate or hyaluronan) are currently studied, very few cationic polysaccharides have been tested for such a purpose. Chitosans represent the typical natural PEs showing a net positive charge at acidic pH values thanks to the protonation of glucosamine (the "D" monomer) amino groups in the C2 position. Chitosan-based complex coacervates have been recently investigated with respect to their physical/chemical and biological properties.[18−21] The use of chitosans is often limited by their poor solubility at neutral pH values, especially for medium/high molecular weight chitosans with fraction (F_A) of acetylated units (the "A" units) < 0.4. Modification of chitosan via grafting of chemical moieties can overcome such limitations. Moreover, the introduction of biologically active groups onto the chitosan backbone can elicit intracellular biochemical signals, via specific ligand−receptor interactions, when the modified chitosan is in contact with eukaryotic cells.[22,23]

In this context, the chemical and biological properties of a lactose-modified chitosan, named CTL, have been widely investigated by our research group. CTL is an operational—albeit rational—name for a member of a family of branched chitosan derivatives obtained after reduction of the Schiff base formed between the amino group of the D units of chitosan—CT—and the reducing end of mono- or disaccharides, like lactose—L, then CTL—or maltose—M, then CTM. CTL (previously also addressed as Chitlac in our scientific publications) was found to favor the aggregation of chondrocytes, to enhance their proliferation, to elicit type II collagen-glycosaminoglycan biosynthesis, and to selectively bind galactose-binding proteins as Galectin 1.[24−26] Moreover, CTL exerted a positive effect on the proliferation of an osteoblast-like cell line and on the osteointegration of thermosets implants.[27] Complex coacervation studies involving CTL and alginate,[14] or CTL in combination with two different polyanions, namely ternary systems CTL-alginate-hyaluronan,[13] have already been proposed, highlighting the pivotal role of ionic strength in the transition from soluble complexes to associative phase separation. In a recent work, a proof-of-concept of the fabrication of nanocoacervates based on CTL and tripolyphosphate (TPP) was given.[28] In the same work, the need to improve the stability of such coacervates has been clearly demonstrated, since it was found that physiological values of pH, ionic strength, and temperature were deleterious for their stability.

Given all above-discussed considerations and based on our previous contribution,[28] in this work we aimed at substituting TPP with a low molecular weight HA, herein envisaged as a polymeric cross-linker for CTL, in order to overcome some of the aforementioned limitations ascribable to TPP usage. Specifically, the ability of CTL (polycation) to promote complex coacervation with hyaluronan (polyanion) is explored for developing spheroidal matrices in the nano-/microsize domain. Then, a systematic investigation about dissolution stability is presented to highlight the usefulness in exploiting HA with respect to TPP for stabilizing the colloids. Finally, the potential application of HA/CTL coacervates as drug carriers and their bioactivity toward a selected cellular model is investigated.

2. MATERIALS AND METHODS

2.1. Materials. Sodium hyaluronate, HA, (with intrinsic viscosity, $[\eta]$, of 270 mL/g and an estimated viscosity-average molecular weight, $\overline{M}_v$, of 90 000, Bioibérica S.A.) was kindly provided by Sigea s.r.l. (Trieste, Italy). Two samples of the hydrochloride form of CTL (CAS Registry Number 2173421-37-7) with different values of the fraction of lactose-modified (*i.e.* *N*-(1-deoxylactit-1-yl)) glucosamine units, F_L, were provided by biopoLife s.r.l. (Trieste, Italy). They had been obtained from two different chitosan batches from Chitoceuticals Heppe Medical Chitosan GmbH, Germany. The viscosity-average molecular weight, $\overline{M}_v$, values of the starting chitosans were 360 000 for CTL47 and 380 000 for CTL60, respectively. According to the determined composition, the corresponding (derived) $\overline{M}_v$ values of the CTL derivatives were 760 000 and 910 000, respectively (see Table 1). The physical−chemical features of CTL samples are summarized in Table 1.

Table 1. Chemical Composition of CTL Samples Used in This Study[a]

CTL sample	F_A	F_D	F_L	$\overline{M}_v$
CTL47	0.12	0.41	0.47	760 000
CTL60	0.07	0.33	0.60	910 000

[a]F_A stands for the fraction of acetylated units, F_D for the fraction of deacetylated units, and F_L for the fraction of lactose-modified units. $\overline{M}_v$ is the viscosity-average molecular mass of the CTL samples, calculated on the basis of the corresponding $\overline{M}_v$ values of the parent chitosans and of the values of F_L.

HEPES buffer, acetic acid, sodium acetate, Percoll, 2-(N-morpholino)ethanesulfonic acid (MES), bovine serum albumin (BSA, Cohn fraction V, ≥96% cell culture-tested), dihydrorhodamine 123 (DHR), horseradish peroxidase (HRP), fluoresceinamine isomer I, dexamethasone, type VI, fibrinogen (FBG) from human plasma, and sodium hydroxide were purchased from Sigma-Aldrich Chemical Co. Hydrochloric acid was purchased from Carlo Erba (Milano, Italy). Deionized Milli-Q water was used throughout. All solutions used in the biological assays were prepared in endotoxin-free water or saline (0.9% w/v NaCl) for clinical use.

2.2. Preparation of Coacervates. CTL and HA solutions were prepared separately by dissolving polymers in deionized filtered water at a final concentration of 1.5 g/L; NaOH 0.1 M or HCl 0.1 M were used to adjust the pH of solutions at 4.5 before mixing. Polymers were then filtered through 0.45 μm filters. The formation of HA/CTL coacervates was achieved by simply dropping HA solution into CTL while gently stirring, with constant total polymer concentration of 1.5 g/L, weight ratio HA/CTL of 0.25, and final volume of 2 mL. The final charge [−]/[+] ratio resulted 0.24 and 0.26 in the case of coacervates prepared with CTL47 and CTL60, respectively. The coacervate suspensions were gently stirred for 20 min at room temperature before performing further analyses. Complex coacervation between CTL and HA was investigated in two different conditions, namely in the absence of supporting salt, i.e. NaCl, or in the presence of NaCl 150 mM. The molar ratio of supporting salt (NaCl) to total buffer (AcOH/AcNa) was kept constant and equal to 15 throughout the measurements.[13]

2.3. Transmittance of Coacervate Solutions. The transmittance of HA/CTL coacervates was measured at a wavelength of 550 nm with an Ultrospec 2100 pro (Bioscience, England). As blank, the transmittance of separate polysaccharides and that of deionized water was measured as well. At least three replicates were recorded for each sample and the results were averaged.

2.4. Characterization of Coacervates. Dynamic Light Scattering (DLS) measurements were performed using a Zetasizer Nano ZS system (Malvern Instruments, Inc., Southborough, MA), in order to evaluate the intensity of 173° scattered light (Derived Count Rate - kilocounts per second, kcps), the average hydrodynamic diameter, and the polydispersity index (PDI) of the coacervates. Coacervates

DOI: 10.1021/acs.biomac.8b00863
Biomacromolecules 2018, 19, 3936−3944

solutions were diluted 1:10 v/v in filtered deionized water (pH 4.5), and DLS measurements were performed at 25 °C, analyzing each sample in triplicate.

The morphology and the size of HA/CTL coacervates were examined by transmission electron microscopy (TEM). 10 μL of colloids (diluted 1:100 v/v using deionized water as solvent) were placed on a carbon film 300 mesh copper grid and air-dried. The sample was stained with 10 μL of a 0.1% w/v uranyl acetate solution for 2 min at room temperature before acquiring images by means of Philips EM 208 microscope, using an accelerating voltage of 100 kV.

2.5. Dissolution Stability as a Function of pH and Time. DLS analyses were performed in order to check the stability of coacervates at different pH values. Specifically, coacervates were formed at pH 4.5 (see paragraph 2.2), and pH increased by addition of NaOH 0.1 M under gentle stirring. The transmittance, *T*, and the light scattered at 173° (i.e., derived count rate) were analyzed for solutions at selected pH values. Coacervates stability was also evaluated by incubating the samples at 37 °C. DLS measurements were performed immediately after the formation of coacervates and after 1, 3, 7, 14, and 21 days of incubation, respectively.

2.6. Effect of Freeze-Drying on Coacervates Stability. The stability of coacervates after freeze-drying was evaluated in both the presence and absence of trehalose as cryoprotectant.[29] Trehalose was solubilized in deionized water (10% w/v final concentration). Coacervates were diluted 1:2 v/v with the cryoprotectant, and the resulting solutions were further diluted 1:5 v/v in deionized water prior to DLS analyses. Samples in the presence/absence of cryoprotectant were placed in 1.5 mL tubes and freeze-dried overnight. Resulting formulations were then suspended in the same volume of buffer, vortexed, and analyzed in triplicate by DLS after dilution 1:5 v/v in deionized water.[28]

2.7. Encapsulation of Model Molecules. Fluoresceinamine isomer I and dexamethasone were selected as model-payloads to determine the encapsulation efficiency and drug loading capacity of the selected formulation. The former molecule was solubilized in methanol (1 mg/mL final concentration) and used to prepare serial dilutions using acetate buffer 10 mM and NaCl 150 mM as the solvent. The linear range of fluorescence intensity as a function of concentration (buffer without fluorophore as blank) was recorded using a BMG LABTECH 96 spectrofluorometer, with λ_{ex} = 485 nm and λ_{em} = 520 nm. The fluorophore was added at a final concentration of 2 μg/mL to 1.5 mL of CTL solutions. In the case of dexamethasone, the final concentration was 20 μg/mL; the absorbance was recorded at λ = 241 nm using a Ultrospec 2100 pro (Bioscience, England). Molecule-loaded coacervates were left 5 min under stirring to homogeneously distribute the payload. Finally, 500 μL of HA were added dropwise and the mixtures stirred for 15 min. 500 μL of the particles solution were placed in 1.5 mL tubes and centrifuged at 9 000*g* for 1 h. After centrifugation, the supernatants were collected and analyzed. The supernatant of coacervates prepared without payload was used as blank. Calibration curves were used to determine the molecules concentration in the supernatant. Encapsulation efficiency (%) was determined according to eq 1:

$$EE = \frac{C_i - C_x}{C_i} \times 100 \quad (1)$$

where C_i corresponds to the initial concentration of the payload, C_x is the payload concentration in the supernatant after sample centrifugation. Loading capacity (expressed as w/w ratio) was determined as eq 2:

$$LC = \frac{w_t - w_x}{w_p} \quad (2)$$

where w_t corresponds to the total mass of the encapsulated molecule, w_x is the mass recovered from the supernatant, and w_p is the mass of coacervates.[30] Payload-loaded samples were also analyzed by DLS to evaluate their hydrodynamic diameter and PDI.

2.8. Release Experiments. The leakage of dexamethasone from HA/CTL47 coacervates was measured in AcOH/AcNa buffer 10 mM as final concentration (pH 4.5, NaCl = 150 mM) at 37 °C. Dexamethasone was encapsulated at a final concentration of 20 μg/mL, and resulting coacervate dispersions were sealed in a dialysis tube (Sigma-Aldrich, cutoff 12 kDa) and placed in 2 mL of the same buffer under shaking conditions. The dialysis solution was collected and replaced with fresh buffer after each time investigated. The amount of dexamethasone was quantified as indicated in paragraph 2.7. The release of dexamethasone from HA/CTL47 coacervates was monitored up to 4 h, and results are reported as the percentage of cumulative release over time.

2.9. Isolation of Human Neutrophils. Venous blood was collected from healthy volunteers after obtaining written informed consent, with the approval of the Institutional Ethical Committee. Neutrophils were isolated by a discontinuous Percoll gradient centrifugation as previously described[31] and suspended in PBS solution, pH 7.4, containing 5 mM glucose and 0.2% BSA. Immediately before use, cell suspensions were washed in MES-buffered saline solution (MBS) containing 140 mM NaCl, 5 mM KCl, 5 mM glucose, 10 mM MES (pH 6.0), and 0.2% BSA (MBS-BSA), and suspended in the same medium.

2.10. Preparation of Fibrinogen-Coated Surfaces. Flat-bottom poly(styrene) wells (F16 MaxiSorp Nunc-Immuno Modules or F16 Black MaxiSorp Fluoronunc Cert, Thermo Fisher Scientific, Roskilde, Denmark) were coated with FBG as described elsewhere.[32] Briefly, 50 μL of a FBG solution (400 μg/mL in PBS) were placed in each well, and the plate was left at 37 °C for 2 h in a humidified chamber. Prior to use, the wells were rinsed three times with PBS.

2.11. Evaluation of H_2O_2 Production. H_2O_2 generation was assessed using DHR.[33,34] Neutrophils (1.25×10^6 cells/mL in MBS-BSA) were loaded with 40 μM DHR for 30 min at 37 °C in a shaking water bath, in the dark. Five to 10 min before starting the assay, the cell suspension was supplemented with 1 mM $CaCl_2$ and 1 mM $MgCl_2$. Then, 60 μL aliquots of this suspension were dispensed into FBG-coated black wells containing the HA/CTL47 coacervates (50–150 μg/mL final concentration) or the same volume of acetate buffer solution, and HRP (1 μg/mL final concentration), in a total volume of 0.15 mL MBS-BSA supplemented with 1 mM $CaCl_2$ and 1 mM $MgCl_2$ (Ca^{2+}/Mg^{2+} MBS-BSA). The plate was incubated at 37 °C in the dark, and, at the desired times, readings were taken with a microplate fluorescence reader (Tecan Infinite F200; Tecan Austria GmbH, Grödig, Austria) at 485 nm (λ_{ex}) and 535 nm (λ_{em}). H_2O_2-independent oxidation of DHR was measured in wells containing DHR-loaded neutrophils pretreated for 10 min with the NADPH-oxidase inhibitor DPI (5 μM final concentration),[35] and the fluorescence values registered at each incubation time were used as a baseline and subtracted from the actual experimental ones.

2.12. Measurement of Neutrophil Adhesion. The number of neutrophils adherent to FBG was assessed by quantifying myeloperoxidase activity as described in Menegazzi et al.[31] Adhesion tests were conducted in FBG-coated transparent wells to monitor cell morphology by light microscopy and were run in parallel and in the same experimental conditions of those used to evaluate H_2O_2 production, except for the omission of DHR and HRP.

2.13. Statistical Analysis. Statistical analysis was performed with Student's *t test,* using GraphPad Prism 5.0 (GraphPad Software, San Diego, CA). *p-values* less than 0.05 were considered statistically significant.

3. RESULTS AND DISCUSSION

3.1. Effect of the Ionic Strength on Complex Coacervation. In a previous contribution we demonstrated that the formation of CTL60-based coacervates using tripolyphosphate (TPP) as the cross-linker was hampered when slight amounts of supporting salt, i.e. NaCl, were mixed with polymer before coacervation.[28]

To evaluate the role played by the ionic strength for the formation of coacervates based on CTL60 and hyaluronan, a single drop-by-drop injection step of the polyanion—i.e.

DOI: 10.1021/acs.biomac.8b00863
Biomacromolecules 2018, 19, 3936−3944

hyaluronan—into CTL60 solution was exploited. The onset of turbidity was noticed instantaneously upon polysaccharides mixing without supporting salt, as demonstrated by turbidity analyses (Figure 1A). It has also to be said that the liquid–liquid phase separation was clearly not accompanied by the presence of very large colloidal precipitates. A further drop in the transmittance—i.e. higher turbidity of the system—was noticed when the synthesis was performed in the presence of NaCl 150 mM (Figure 1A), still without precipitates. The present finding was not of surprise since the increase of turbidity following salt addition—up to some extent—is a typical behavior of nonstoichiometric polyelectrolyte complexes.[36,37] Furthermore, our results nicely corroborated those of Kayitmazer and co-workers, who identified a similar behavior using chitosan and hyaluronan as polyelectrolytes to promote complex coacervation.[19]

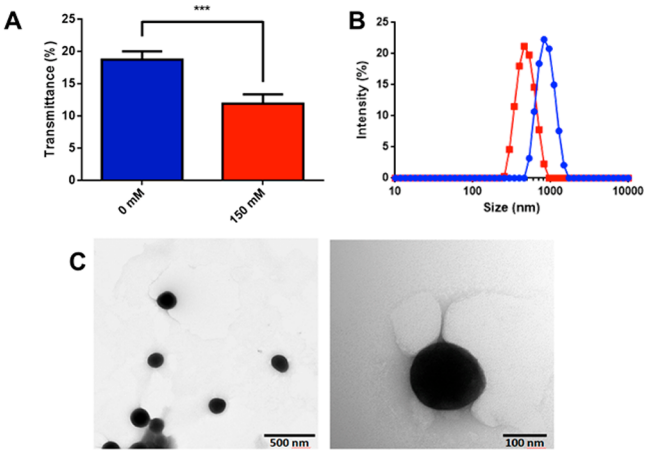

Figure 1. (A) Influence of the ionic strength on the transmittance of coacervate solutions prepared at pH 4.5, dropping hyaluronan into CTL60 solutions. Results are reported as mean (±SD, n = 5). Statistical analysis: coacervates formed without NaCl vs coacervates formed in the presence of NaCl 150 mM: Student's t-test: ***, $p < 0.001$. (B) DLS investigation on the influence of ionic strength on coacervates formation. Size distribution of formulations prepared without supporting salt (blue) and with NaCl 150 mM (red). (C) TEM images of coacervates synthesized in the presence of NaCl 150 mM and subsequently diluted 1:100 v/v in deionized water to acquire images.

To give further insights into the complex coacervation between hyaluronan and CTL60, dynamic light scattering analyses were carried out on the same samples (Figure 1B). The size distributions by intensity indicate a unimodal curve profile for coacervates synthesized both without supporting salt and in the presence of NaCl 150 mM, thus suggesting that a homogeneous ensemble of (spherical) scatters was present. Strikingly, a significant shift toward smaller size values was noticed in the latter case, with the hydrodynamic diameter passing from 980 ± 90 nm to 454 ± 29 nm. Again, our results are in line with what was found by Kayitmazer and co-workers.[19] Specifically, in the quoted paper the authors identified a decrement of colloids dimension following the increase of the ionic strength up to 0.15 M; beyond this value, an abrupt coacervates size increase was detected. Though the latter behavior may be reasonably interpreted in terms of large clusters formation due to the vanishing of electrostatic repulsions among smaller colloids, the reduction of coacervates dimensions in the presence of 150 mM NaCl should conversely take into account the simple role played by the ionic strength in reducing the (overall) hydrodynamic diameter of both the macromolecules. It is therefore expected that CTL and HA would assemble in smaller, more compact, and homogeneous coacervates. As expected, the homogeneity of the system increased in the presence of the supporting salt, showing a significant decrease of the polydispersity index (PDI) from 0.27 ± 0.02 for the coacervates fabricated without supporting salt to 0.14 ± 0.03 for those formed in NaCl 150 mM.

Sample-case transmission electron microscopy (TEM) images of coacervates synthesized in the presence of NaCl 150 mM corroborated the spherical shape of colloids and their good homogeneity (Figure 1C).

Finally, it is important to underline that CTL60 and HA not only were able to form spherical and homogeneous coacervates in the presence of high salt content, but even that the formation of coacervates occurred immediately after the polymer dropping, without any phase separation lag or equilibration times. These results highlight an important difference between simple coacervation (i.e., involving one macromolecule) and complex coacervation (involving two or more macromolecules): indeed, the ionotropic gelation of chitosan and its derivative CTL using tripolyphosphate (TPP) as cross-linker is drastically hampered by elevated NaCl (i.e., 150 mM) and low TPP amounts,[38,28] mostly in the first stage

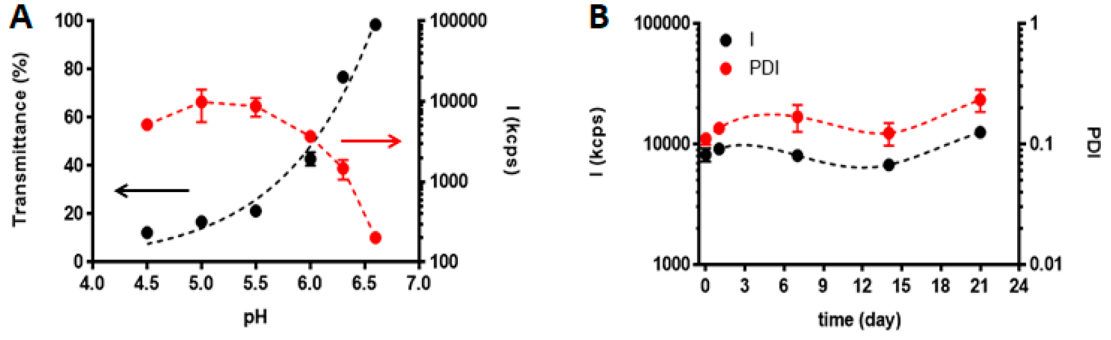

Figure 2. (A) Dissolution stability of HA/CTL60 coacervates as a function of pH: transmittance (black dots) and intensity of 173° scattered light (red dots) recorded from DLS measurements: dashed lines are drawn to guide the eye. (B) Dissolution stability of HA/CTL60 coacervates as a function of time. 173° scattered light (black dots) and polydispersity index—PDI—(red dots). Coacervates were kept at 37 °C for 21 days and DLS measurements performed at selected timepoints; dashed lines are drawn to guide the eye. All results are reported as mean (±SD, n = 3).

DOI: 10.1021/acs.biomac.8b00863
Biomacromolecules 2018, 19, 3936−3944

of macromolecular assembly. Hence, the use of hyaluronan—presently envisaged as a low MW "cross-linker" for CTL—in fostering the formation of complex coacervates in physiological osmolarity is more effective than the multivalent anion TPP.

3.2. Coacervates Dissolution Stability as a Function of pH and Time. The stability of coacervates as a function of pH and time was studied thereafter. Transmittance studies pointed at constant values for T (below 40%) up to pH 5.5; beyond that, an increase of T of about 20% marked the initial instability of the system (Figure 2A). Moreover, the formation of visible aggregates was detected above pH 6.3. The complete dissolution of coacervates was noticed in the high pH range, as noticed by T values reaching those of disentangled polymers. The opposite trend of the scattering intensity data at 173° reported in the same figure validated the instability of the system at pH $\geq$ 6. Specifically, a sudden decrement of scattering intensity paralleled by an increase of T was observed at pH > 6, thus pointing at the onset of coacervates dissolution. The polydispersity index computed from DLS supported the transition from almost homogeneous colloids (PDI = 0.14 ± 0.03) to aggregates with variable dimensions (PDI = 0.48 ± 0.20). It can be concluded that coacervates largely dissolve in a range of pH 6.0−6.3, even if the presence of residual chain aggregates cannot be excluded given the residual scattering intensity.

Coacervates stability was then studied as a function of time at 37 °C and pH = 4.5. An almost constant profile of scattering intensity was observed up to 14 days of incubation (Figure 2B). A slight increase of both derived count rate and PDI occurred after 3 weeks at 37 °C, indicating a reasonable swelling or partial aggregation of the coacervates. Size distribution curves were almost comparable after 21 days of incubation (data not shown); moreover, the absence of visible aggregates indicated that coacervates remained stable throughout the experiment. This result is at variance with the CTL/TPP case, indicating that the use of hyaluronan provides an additional benefit with respect to TPP.[28] Indeed, the replacement of the multivalent anion with low molecular weight hyaluronan produced stable particles at physiological temperature.

To further improve the stability of coacervates against dissolution at slightly acidic pH values tending to neutrality, the hypothesis to use CTL samples with different fraction of lactose-modified units (F_L) was considered. CTL samples having different F_L values present different fraction of both primary and secondary amines, meaning that they would be differently influenced by pH variation. Indeed, the calculated pK_a values for primary and secondary amines were 6.69 and 5.87, respectively.[39] It is therefore expected that CTL samples endowed with a lower degree of substitution would better withstand the pH increase from 5.5 to 6.5. Hence, a second CTL sample with F_L = 0.47, CTL47, was used to form coacervates. The comparison of the size intensity distributions for the two types of formulations is reported in Figure 3A. The two different formulations peak at almost identical size (HA/CTL60 = 454 ± 29 nm, HA/CTL47 = 461 ± 67 nm) and show a very similar (Gaussian-like) distribution. This finding clearly indicates that a 13% difference in the values of lactitol branching and the slight discrepancy in terms of CTL molecular weight did not greatly influence the formation and the homogeneity of coacervates. At variance, it seems that the almost identical charge [−]/[+] ratio—i.e. 0.24 and 0.26 in the case of coacervates prepared with CTL47 and CTL60, respectively—contributes to such a similar behavior.

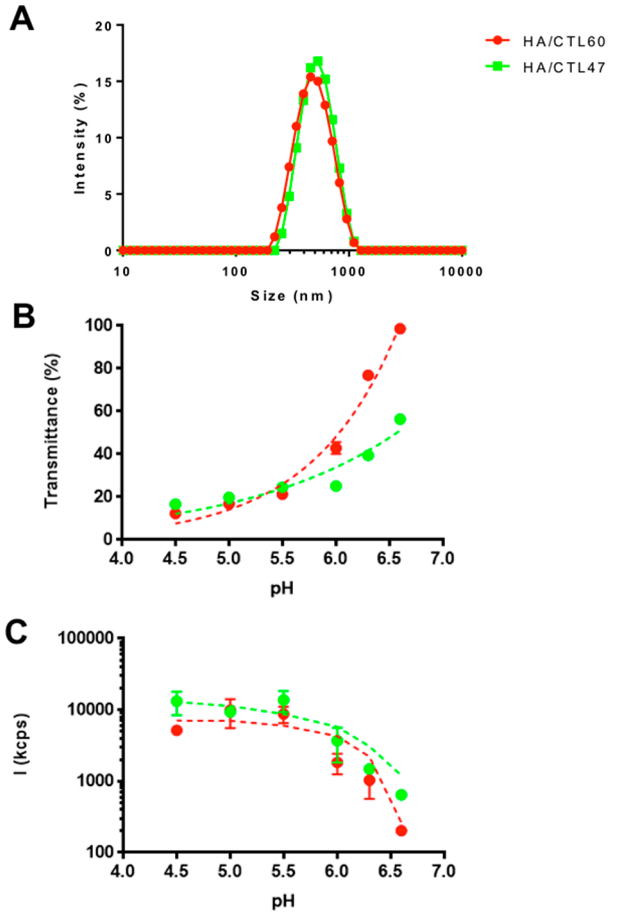

Figure 3. (A) DLS size distribution curves of coacervates synthesized with different CTL samples. All formulations were prepared at pH 4.5, AcOH/AcNa buffer 10 mM and NaCl = 150 mM. Dissolution stability as a function of pH: (B) transmittance and (C) DLS analyses. Color legend: HA/CTL60 (red dots) and HA/CTL47 (green dots). Results are reported as mean (±SD, n = 3). Dashed lines are drawn to guide the eye.

The pH profile of the turbidity of the HA/CTL47 system paralleled that of HA/CTL60, transmittance, T, increasing with increasing pH. However, for pH = 6.0 and beyond, the T values of the systems containing CTL47 showed a progressively lower value of T, up to pH 6.3, for which T = 39.4 ± 0.4 for F_L = 0.47 and T = 76.9 ± 1.3 for CTL with F_L = 0.60. This finding was also supported by DLS analysis, where, although the scattering intensity decreased in a similar fashion, the data of the systems based on CTL47 always showed intensity values larger than those of the CTL60 systems (Figure 3C). Hence, the stability against dissolution can be improved by decreasing the fraction of lactose-modified units from 0.60 to 0.47. By further increasing pH, it was found that coacervates made of F_L = 0.47 CTL remained stable at pH 6.6 for approximately 40 min, whereas a complete dissolution of the system occurred subsequently, suggesting that a kinetically controlled effect is also involved in the dissolution of coacervates. Finally, the time-stability at 37 °C and pH = 4.5 was verified up to 21 days for the latter formulation, showing a very similar behavior if compared with F_L = 0.60 counterparts (data not shown).

DOI: 10.1021/acs.biomac.8b00863
Biomacromolecules 2018, 19, 3936−3944

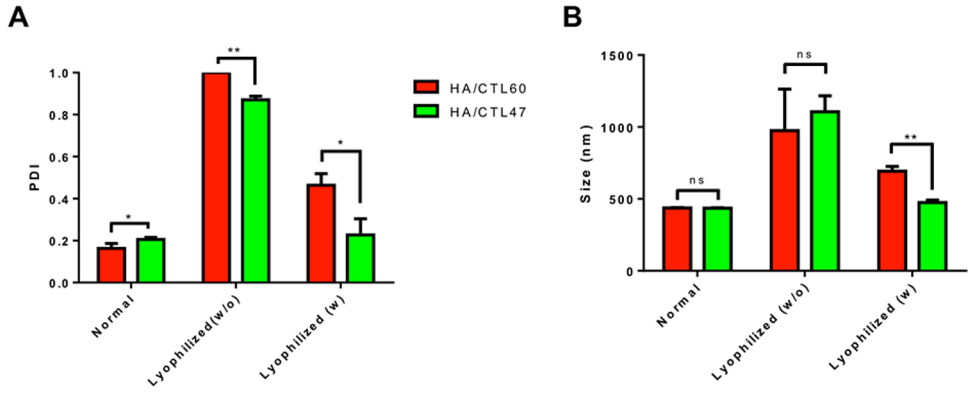

Figure 4. Storage stability of coacervates. PDI (A) and average hydrodynamic diameter (B). Coacervates were analyzed before (Normal) and after the freeze-drying process in the presence (Lyophilized—w) or absence (Lyophilized—w/o) of trehalose. Color legend: HA/CTL60 (red), HA/CTL47 (green). Results are reported as mean (±SD, $n = 3$). Statistical analysis: HA/CTL60 vs HA/CTL47. Student's t-test: *, $p < 0.05$; **, $p < 0.01$; NS, not significant.

3.3. Coacervates Stability upon Freeze-Drying, Encapsulation of Model Molecules, and in Vitro Release. The possibility to freeze-dry suspensions of coacervates for long storage purposes was investigated. DLS results obtained on both freshly prepared and dried coacervates are reported in Figure 4. Both formulations, i.e. with $F_L = 0.60$ or $F_L = 0.47$, were freeze-dried in the presence or absence of trehalose as cryoprotectant.[29] The results in Figure 4A indicate that freeze-drying without trehalose brought about a massive and uncontrolled aggregation of particles. The presence of trehalose was beneficial for the impact of the freeze-drying process for both F_L values. The values of both PDI and intensity showed a net benefit using trehalose as a cryoprotectant. In particular, coacervates based on CTL47 and containing trehalose showed both PDI and intensity values after freeze-drying practically equal to the corresponding values before freeze-drying. DLS analyses clearly proved that the use of trehalose as cryoprotectant is necessary for the storage of HA/CTL coacervates. The present results differ from what was reported in our previous contribution for simple coacervation systems based on CTL60 and TPP, where the presence of trehalose resulted as detrimental for the freeze-drying process.[28] This difference could stem from a different alignment of the polycationic (CTL) part with the polyanionic counterpart in the case of TPP with respect to HA. Possibly, in the former case, the much shorter dimension of the cross-linking agent could leave a large number of lactitol side-chains still free to interact with water ensuring an antifreezing effect. The observation that, in such conditions, the addition of trehalose is detrimental for the coacervate integrity might suggest a sort of "competition" between the lactitol side-chains and the added trehalose with respect to the ability of interfering with water-freezing. At variance, in the latter case the longer stretch of the polymeric arrangement could immobilize longer lactitol-containing sequences of CTL, thus canceling their potential of interference with water-ordering (and crystallization) upon freeze-drying. As a result, the addition of trehalose could act as a restoring agent of the antifreezing potential of the intact CTL moiety.

The effect of the lactitol content on both PDI and dimension of coacervates was of interest. Whereas in the case of CTL47 the proposed polycation/polyanion alignment seemed to cancel the lactitol effect on water crystallization in the absence of trehalose, the addition of the latter seemed to be able to restore the antifreeze effect. At variance, in the case of CTL60 the larger amount of lactitol partially counterbalanced the positive effect of the addition of trehalose as suggested by the fact that with trehalose neither PDI nor dimensions reattain the values of the "normal" condition, providing an indirect support to the hypothesis of a "competition" between lactitol and trehalose in their antifreeze ability.

The ability of coacervates to encapsulate proper payloads was investigated to consider them as potential drug delivery systems. Fluoresceinamine isomer I was used at first as model molecule and the synthesis of coacervates was performed as described in paragraph 2.7. CTL samples at two different F_L values formed coacervates with similar dimensions and homogeneity even when hosted the payload, as detected by DLS analysis (data not shown). The two formulations showed an identical ability to encapsulate fluoresceinamine isomer I (Table 2). The calculated loading capacity was 0.65 μg payload/mg carrier, with an encapsulation efficiency around 96%, which is in line with similar systems.[40,41] The encapsulation efficiency and drug loading for HA/CTL47 coacervates were verified also using dexamethasone as payload, yielding 56 ± 1% and 3.74 ± 0.07 μg payload/mg carrier, respectively.

Table 2. Encapsulation Efficiency and Loading Capacity of Coacervates Prepared with Hyaluronan and CTL at Different Fractions of Lactose-Modified Units (F_L)[a]

Payload	Sample	Encapsulation Efficiency (%)	Loading Capacity (μg/mg)
Fluoresceinamine	HA/CTL60	97 ± 6	0.65 ± 0.04
	HA/CTL47	98 ± 5	0.65 ± 0.03
Dexamethasone	HA/CTL47	56 ± 1	3.74 ± 0.07

[a]Conditions: synthesis at pH 4.5, NaCl = 150 mM, room temperature.

In vitro release experiments were undertaken to study the leakage of dexamethasone from HA/CTL47 coacervates, and results are reported in Figure 5. The release profile of the payload over time was almost constant up to 1 h of incubation, with around 80% of total drug released. After longer incubation time, the release profile tended to reach a plateau with almost total dexamethasone released during 4 h of incubation. Overall, our findings demonstrated that HA/CTL47 coacervates were

DOI: 10.1021/acs.biomac.8b00863
Biomacromolecules 2018, 19, 3936−3944

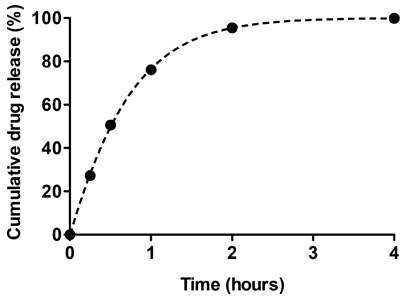

Figure 5. Cumulative release of dexamethasone from HA/CTL47 coacervates. Conditions: AcOH/AcNa buffer 10 mM, NaCl = 150 mM, pH 4.5, T = 37 °C. The results are reported as mean (±SD, n = 3). Dashed line is drawn to guide the eye.

able to gradually release the selected payload in the early stages of incubation.

3.4. Effect of Coacervates on Neutrophils Activity. Both HA/CTL60 and HA/CTL47 systems resulted to be unstable at neutral pH. However, the HA/CTL47 system proved to be reasonably stable at acidic pH, namely at pH 6. Extracellular acidosis is a condition commonly associated with inflammatory processes, where extracellular pH values as low as 6.1 have been documented.[42,43] Moreover, acidic pH values were found in the cancer microenvironment.[44] pH-dependent features of chitosan/hyaluronic acid-based nanoparticles have been a matter of investigation by other authors.[40,45] In view of its potential use *in vivo* as a drug carrier, the HA/CTL47 system was selected to perform *in vitro* experiments in acidic pH conditions, namely pH 6.0. We decided to evaluate the effect of CTL47-based coacervates on neutrophils, which represent a key first-line defense of the immune system. Specifically, the possibility that coacervates could modulate the generation of H_2O_2 and/or the adhesion of neutrophils to FBG was tested.

Figure 6A shows that coacervates, at the tested concentrations, had only a minor stimulatory effect on the basal production of H_2O_2 by human neutrophils at pH 6.0. However, the coacervates elicited a marked increase in the number of cells adherent to FBG (Figure 6B), which was accompanied by an exacerbation of the elongated morphology exhibited by neutrophils at this pH value.

The expected increase in cell adherence stimulated by HA/CTL47 prompted us to replot the data obtained in the DHR assay and normalize them on the basis of cell adhesion (Figure 6C). Surprisingly, the new plotting unraveled that the increased number of adhered cells, as a whole, produced a lower amount of H_2O_2 than control neutrophils incubated in the absence of the coacervates. Such a reduction of H_2O_2 generation could be explained by a HA/CTL47-mediated scavenging effect, since both HA and chitosan, from which CTL is obtained, have been shown to be efficient ROS scavengers.[41,42] Moreover, we have recently demonstrated that chitosan/HA nanoparticles are capable of scavenging O_2^-/H_2O_2 released by neutrophils.[17] Taking the cue from some literature data, additional hypotheses to explain the effect of HA/CTL47 on adherence and/or ROS production could be proposed. The former one calls in the possibility that the interaction between neutrophils and the coacervates, involving as-yet unidentified surface receptor(s), somehow enhances the affinity of β_2 integrins, thereby improving neutrophil adherence to FBG.[46] Such an increased adherence would then trigger

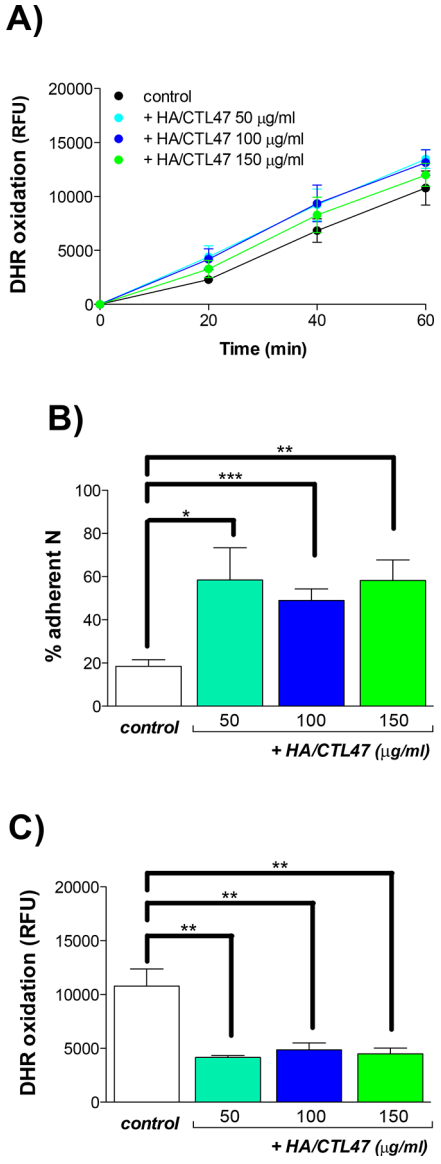

Figure 6. Effect of HA/CTL47 coacervates on neutrophil H_2O_2 production and adhesion to fibrinogen (FBG). The coacervates were prepared at pH 4.5. The pH was then raised to 6.0 before performing biological experiments. (A) Time-course of H_2O_2 generation. Dihydrorhodamine 123 (DHR)-loaded neutrophils (suspended in Ca^{2+}/Mg^{2+} MBS-BSA) were incubated at 37 °C in the absence or presence of coacervates, in FBG-coated wells containing horseradish peroxidase (HRP). H_2O_2 production was evaluated by fluorometric measurement of oxidized DHR. Data are means (±SE) of two triplicate experiments. (B) Adhesion of neutrophils to FBG. Adhesion was quantified after 60 min of incubation by measuring myeloperoxidase activity as detailed in the Materials and Methods. Data are means (±SE) of two triplicate experiments. (C) H_2O_2 production at 60 min of incubation. Results reported in (A) have been normalized for the number of adherent cells (B). Statistical analysis: coacervates-treated neutrophils vs control neutrophils. Student's t-test: *, $p < 0.05$; **, $p < 0.01$; ***, $p < 0.001$.

intracellular signals which downregulate ROS production, similarly to what has been described to occur after the interaction of $\alpha_v\beta_3$ integrin with fibronectin.[47] As a latter alternative, the contact of HA/CTL47 with neutrophils could signal for an improved activity of ROS degradative enzymes, such as catalase and superoxide dismutase, thus resembling the

DOI: 10.1021/acs.biomac.8b00863
Biomacromolecules 2018, 19, 3936−3944

quercetin-mediated effect that has been documented in a model of neuroinflammation using a human neuroblastoma cell line.[48] Clearly, specific investigation is additionally required to clarify this interesting point.

4. CONCLUSIONS

The preparation of HA/CTL-based coacervates *via* electrostatic complex coacervation has been reported in this work. The results showed that spheroidal nano-/microparticles could be obtained when HA was added to CTL in the presence of a physiological concentration (i.e., 150 mM) of NaCl, thereby overcoming screening phenomena. Interestingly, it was not only found that the supporting salt was unable to completely screen electrostatic attractive interactions, but it was even showed that it helped the reduction of the size distribution of coacervates. Time dissolution stability studies proved that coacervates did not dissolve at 37 °C up to 3 weeks; conversely, they disentangled upon increasing pH toward neutrality. Interestingly, the rate of dissolution could be tuned, to some extent, by varying CTL chemical composition, thus proving the usefulness of exploiting HA for stabilizing CTL-based colloids, with respect to and at variance with tripolyphosphate (TPP). The selected systems displayed suitable encapsulation efficiency, exhibited optimal drug loading, and preserved physical properties after freeze-drying in the presence of trehalose as cryoprotectant. Biological experiments using human neutrophils as cellular model pointed out the ability of HA/CTL coacervates to exert a significant ROS scavenging activity. Overall, the present findings—together with the documented bioactivity of CTL—suggest that the complex coacervation between CTL and low molecular weight hyaluronan can be considered as an effective strategy to form bioactive carriers to be used for the delivery of drugs toward confined inflamed sites known to be commonly associated with extracellular acidosis.

AUTHOR INFORMATION

Corresponding Author

*E-mail: psacco@units.it. Phone: +39-040-5588733.

ORCID

Pasquale Sacco: 0000-0002-4483-5099

Davide Porrelli: 0000-0002-6437-7646

Ivan Donati: 0000-0003-3752-8346

Notes

The authors declare no competing financial interest.

ACKNOWLEDGMENTS

This study was supported by the INTERREG V-A ITALIA-SLOVENIA 2014-2020 BANDO 1/2016 ASSE 1 - project BioApp 1472551605. The authors also acknowledge the support in part by the ERA-MarineBiotech project Mar3Bio.

REFERENCES

(1) Lapitsky, Y. Ionically crosslinked polyelectrolyte nanocarriers: Recent advances and open problems. *Curr. Opin. Colloid Interface Sci.* **2014**, *19*, 122−130.

(2) de Kruif, C. G.; Weinbreck, F.; de Vries, R. Complex coacervation of proteins and anionic polysaccharides. *Curr. Opin. Colloid Interface Sci.* **2004**, *9*, 340−349.

(3) Kizilay, E.; Kayitmazer, A. B.; Dubin, P. L. Complexation and coacervation of polyelectrolytes with oppositely charged colloids. *Adv. Colloid Interface Sci.* **2011**, *167*, 24−37.

(4) Weinbreck, F.; de Vries, R.; Schrooyen, P.; de Kruif, C. G. Complex Coacervation of Whey Proteins and Gum Arabic. *Biomacromolecules* **2003**, *4*, 293−303.

(5) Chollakup, R.; Smitthipong, W.; Eisenbach, C. D.; Tirrell, M. Phase Behavior and Coacervation of Aqueous Poly(acrylic acid)−Poly(allylamine) Solutions. *Macromolecules* **2010**, *43*, 2518−2528.

(6) Antonov, M.; Mazzawi, M.; Dubin, P. L. Entering and Exiting the Protein−Polyelectrolyte Coacervate Phase via Nonmonotonic Salt Dependence of Critical Conditions. *Biomacromolecules* **2010**, *11*, 51−59.

(7) Chollakup, R.; Beck, J. B.; Dirnberger, K.; Tirrell, M.; Eisenbach, C. D. Polyelectrolyte molecular weight and salt effects on the phase behavior and coacervation of aqueous solutions of poly(acrylic acid) sodium salt and poly(allylamine) hydrochloride. *Macromolecules* **2013**, *46*, 2376−2390.

(8) Malmo, J.; Sørgård, H.; Vårum, K. M.; Strand, S. P. siRNA delivery with chitosan nanoparticles: Molecular properties favoring efficient gene silencing. *J. Controlled Release* **2012**, *158*, 261−268.

(9) Malmo, J.; Vårum, K. M.; Strand, S. P. Effect of Chitosan Chain Architecture on Gene Delivery: Comparison of Self-Branched and Linear Chitosans. *Biomacromolecules* **2011**, *12*, 721−729.

(10) Strand, S. P.; et al. Molecular design of chitosan gene delivery systems with an optimized balance between polyplex stability and polyplex unpacking. *Biomaterials* **2010**, *31*, 975−987.

(11) Li, Y.; et al. Complex Coacervation-Integrated Hybrid Nanoparticles Increasing Plasmid DNA Delivery Efficiency *in Vivo*. *ACS Appl. Mater. Interfaces* **2016**, *8*, 30735−30746.

(12) Black, K. A.; et al. Protein Encapsulation via Polypeptide Complex Coacervation. *ACS Macro Lett.* **2014**, *3*, 1088−1091.

(13) Donati, I.; et al. Polysaccharide-Based Polyanion−Polycation−Polyanion Ternary Systems. A Preliminary Analysis of Interpolyelectrolyte Interactions in Dilute Solutions. *Biomacromolecules* **2011**, *12*, 4044−4056.

(14) Donati, I.; Borgogna, M.; Turello, E.; Cesàro, A.; Paoletti, S. Tuning Supramolecular Structuring at the Nanoscale Level: Non-stoichiometric Soluble Complexes in Dilute Mixed Solutions of Alginate and Lactose-Modified Chitosan (Chitlac). *Biomacromolecules* **2007**, *8*, 1471−1479.

(15) Deng, X.; et al. Hyaluronic acid-chitosan nanoparticles for co-delivery of MiR-34a and doxorubicin in therapy against triple negative breast cancer. *Biomaterials* **2014**, *35*, 4333−44.

(16) de la Fuente, M.; Seijo, B.; Alonso, M. J. Novel hyaluronic acid-chitosan nanoparticles for ocular gene therapy. *Invest. Ophthalmol. Visual Sci.* **2008**, *49*, 2016−24.

(17) Sacco, P.; et al. Butyrate-Loaded Chitosan/Hyaluronan Nanoparticles: A Suitable Tool for Sustained Inhibition of ROS Release by Activated Neutrophils. *Macromol. Biosci.* **2017**, *17*, 1700214.

(18) Lalevée, G.; et al. Highly stretchable hydrogels from complex coacervation of natural polyelectrolytes. *Soft Matter* **2017**, *13*, 6594−6605.

(19) Kayitmazer, A. B.; Koksal, A. F.; Kilic Iyilik, E. Complex coacervation of hyaluronic acid and chitosan: effects of pH, ionic strength, charge density, chain length and the charge ratio. *Soft Matter* **2015**, *11*, 8605−12.

(20) Lalevée, G.; et al. Polyelectrolyte complexes via desalting mixtures of hyaluronic acid and chitosan—Physicochemical study and structural analysis. *Carbohydr. Polym.* **2016**, *154*, 86−95.

(21) Karabiyik Acar, O.; Kayitmazer, A. B.; Torun Kose, G. Hyaluronic Acid/Chitosan Coacervate-Based Scaffolds. *Biomacromolecules* **2018**, *19*, 1198−1211.

(22) Alves, N. M.; Mano, J. F. Chitosan derivatives obtained by chemical modifications for biomedical and environmental applications. *Int. J. Biol. Macromol.* **2008**, *43*, 401−414.

(23) Kim, T. H.; Nah, J. W.; Cho, M.-H.; Park, T. G.; Cho, C. S. Receptor-Mediated Gene Delivery into Antigen Presenting Cells Using Mannosylated Chitosan/DNA Nanoparticles. *J. Nanosci. Nanotechnol.* **2006**, *6*, 2796−2803.

DOI: 10.1021/acs.biomac.8b00863
Biomacromolecules 2018, 19, 3936−3944

(24) Donati, I.; et al. The aggregation of pig articular chondrocyte and synthesis of extracellular matrix by a lactose-modified chitosan. *Biomaterials* **2005**, *26*, 987−98.
(25) Marcon, P.; et al. The role of Galectin-1 in the interaction between chondrocytes and a lactose-modified chitosan. *Biomaterials* **2005**, *26*, 4975−84.
(26) Marsich, E.; et al. Alginate/lactose-modified chitosan hydrogels: a bioactive biomaterial for chondrocyte encapsulation. *J. Biomed. Mater. Res., Part A* **2008**, *84*, 364−76.
(27) Travan, A.; et al. Polysaccharide-Coated Thermosets for Orthopedic Applications: From Material Characterization to In Vivo Tests. *Biomacromolecules* **2012**, *13*, 1564−1572.
(28) Furlani, F.; Sacco, P.; Marsich, E.; Donati, I.; Paoletti, S. Highly monodisperse colloidal coacervates based on a bioactive lactose-modified chitosan: From synthesis to characterization. *Carbohydr. Polym.* **2017**, *174*, 360−368.
(29) Rampino, A.; Borgogna, M.; Blasi, P.; Bellich, B.; Cesàro, A. Chitosan nanoparticles: Preparation, size evolution and stability. *Int. J. Pharm.* **2013**, *455*, 219−228.
(30) Li, H.; et al. Enhancement of gastrointestinal absorption of quercetin by solid lipid nanoparticles. *J. Controlled Release* **2009**, *133*, 238−244.
(31) Menegazzi, R.; Busetto, S.; Dri, P.; Cramer, R.; Patriarca, P. Chloride ion efflux regulates adherence, spreading, and respiratory burst of neutrophils stimulated by tumor necrosis factor-α (TNF) on biologic surfaces. *J. Cell Biol.* **1996**, *135*, 511−522.
(32) Dri, P.; Cramer, R.; Spessotto, P.; Romano, M.; Patriarca, P. Eosinophil activation on biologic surfaces. Production of O2- in response to physiologic soluble stimuli is differentially modulated by extracellular matrix components and endothelial cells. *J. Immunol.* **1991**, *147*, 613−20.
(33) Rinaldi, M.; Moroni, P.; Paape, M. J.; Bannerman, D. D. Evaluation of assays for the measurement of bovine neutrophil reactive oxygen species. *Vet. Immunol. Immunopathol.* **2007**, *115*, 107−125.
(34) Mauch, L.; et al. Chronic granulomatous disease (CGD) and complete myeloperoxidase deficiency both yield strongly reduced dihydrorhodamine 123 test signals but can be easily discerned in routine testing for CGD. *Clin. Chem.* **2007**, *53*, 890−896.
(35) Ellis, J. A.; Mayer, S. J.; Jones, O. T. The effect of the NADPH oxidase inhibitor diphenyleneiodonium on aerobic and anaerobic microbicidal activities of human neutrophils. *Biochem. J.* **1988**, *251*, 887−91.
(36) Volkova, I. F.; Gorshkova, M. Y.; Izumrudov, V. A. Water-soluble nonstoichiometric polyelectrolyte complexes of chitosan with a polystyrenesulfonate anion. *Polym. Sci., Ser. A* **2008**, *50*, 971−976.
(37) Priftis, D.; Megley, K.; Laugel, N.; Tirrell, M. Complex coacervation of poly(ethylene-imine)/polypeptide aqueous solutions: Thermodynamic and rheological characterization. *J. Colloid Interface Sci.* **2013**, *398*, 39−50.
(38) Huang, Y.; Lapitsky, Y. Salt-assisted mechanistic analysis of chitosan/tripolyphosphate micro- and nanogel formation. *Biomacromolecules* **2012**, *13*, 3868−76.
(39) D'Amelio, N.; et al. Insight into the molecular properties of Chitlac, a chitosan derivative for tissue engineering. *J. Phys. Chem. B* **2013**, *117*, 13578−87.
(40) Lallana, E.; et al. Chitosan/Hyaluronic Acid Nanoparticles: Rational Design Revisited for RNA Delivery. *Mol. Pharmaceutics* **2017**, *14*, 2422−2436.
(41) Martins, A. F.; de Oliveira, D. M.; Pereira, A. G. B.; Rubira, A. F.; Muniz, E. C. Chitosan/TPP microparticles obtained by microemulsion method applied in controlled release of heparin. *Int. J. Biol. Macromol.* **2012**, *51*, 1127−1133.
(42) Edlow, D. W.; Sheldon, W. H. The pH of inflammatory exudates. *Exp. Biol. Med.* **1971**, *137*, 1328−32.
(43) Boots, R. H.; Cullen, G. E. The hydrogen ion concentration of joint exudates in rheumatic fever and other forms of arthritis. *J. Exp. Med.* **1922**, *36*, 405−14.
(44) Wike-Hooley, J. L.; Haveman, J.; Reinhold, H. S. The relevance of tumour pH to the treatment of malignant disease. *Radiother. Oncol.* **1984**, *2*, 343−66.
(45) Zaki, N. M.; Nasti, A.; Tirelli, N. Nanocarriers for cytoplasmic delivery: cellular uptake and intracellular fate of chitosan and hyaluronic acid-coated chitosan nanoparticles in a phagocytic cell model. *Macromol. Biosci.* **2011**, *11*, 1747−60.
(46) Nathan, C.; et al. Cytokine-induced respiratory burst of human neutrophils: dependence on extracellular matrix proteins and CD11/CD18 integrins. *J. Cell Biol.* **1989**, *109*, 1341−9.
(47) Lin, L.-J.; et al. The antagonistic roles of PDGF and integrin $\alpha v\beta 3$ in regulating ROS production at focal adhesions. *Biomaterials* **2013**, *34*, 3807−3815.
(48) Bahar, E.; Kim, J.-Y.; Yoon, H. Quercetin Attenuates Manganese-Induced Neuroinflammation by Alleviating Oxidative Stress through Regulation of Apoptosis, iNOS/NF-κB and HO-1/Nrf2 Pathways. *Int. J. Mol. Sci.* **2017**, *18*, 1989.

DOI: 10.1021/acs.biomac.8b00863
Biomacromolecules 2018, 19, 3936−3944